Amyloid seeds formed by cellular uptake, concentration, and aggregation of the amyloid-beta peptide

Xiaoyan Hu[a,1], Scott L. Crick[b,1], Guojun Bu[c], Carl Frieden[d,2], Rohit V. Pappu[b], and Jin-Moo Lee[a,3]

[a]Hope Center for Neurological Disorders and Department of Neurology, [b]Department of Biomedical Engineering and Center for Computational Biology, and [c]Department of Pediatrics, Cell Biology and Physiology, and [d]Department of Biochemistry and Molecular Biophysics, Washington University School of Medicine, St. Louis, MO 63110

Contributed by Carl Frieden, October 2, 2009 (sent for review April 6, 2009)

One of the neuropathological hallmarks of Alzheimer's disease (AD) is the amyloid plaque, primarily composed of aggregated amyloid-beta (Aβ) peptide. In vitro, Aβ_{1-42}, the major alloform of Aβ found in plaques, self-assembles into fibrils at micromolar concentrations and acidic pH. Such conditions do not exist in the extracellular fluid of the brain where the pH is neutral and Aβ concentrations are in the nanomolar range. Here, we show that extracellular soluble Aβ (sAβ) at concentrations as low as 1 nM was taken up by murine cortical neurons and neuroblastoma (SHSY5Y) cells but not by human embryonic kidney (HEK293) cells. Following uptake, Aβ accumulated in Lysotracker-positive acidic vesicles (likely late endosomes or lysosomes) where effective concentrations (>2.5 μM) were greater than two orders of magnitude higher than that in the extracellular fluid (25 nM), as quantified by fluorescence intensity using laser scanning confocal microscopy. Furthermore, SHSY5Y cells incubated with 1 μM Aβ_{1-42} for several days demonstrated a time-dependent increase in intracellular high molecular weight (HMW) (>200 kDa) aggregates, which were absent in cells grown in the presence of Aβ_{1-40}. Homogenates from these Aβ_{1-42}-loaded cells were capable of seeding amyloid fibril growth. These results demonstrate that Aβ can be taken up by certain cells at low physiologically relevant concentrations of extracellular Aβ, and then concentrated into endosomes/lysosomes. At high concentrations, vesicular Aβ aggregates to form HMW species which are capable of seeding amyloid fibril growth. We speculate that extrusion of these aggregates may seed extracellular amyloid plaque formation during AD pathogenesis.

amyloid fibrils | late endosomes | lysosomes | plaques

Alzheimer's disease (AD), the most common form of dementia in Western countries, involves progressive accumulation of amyloid deposits, neuronal loss, cognitive decline, and eventual death. Senile plaques, a key pathological feature of this disease, are composed primarily of the amyloid-beta (Aβ) peptide, and are found throughout the brain (1). Aβ (ranging in length from 39–42 amino acids) is derived from the proteolytic cleavage of an endogenous transmembrane protein known as the amyloid precursor protein (APP). The most common Aβ peptide found in senile plaques is the 42-residue peptide (Aβ_{1-42}) (2), which also shows the strongest propensity for spontaneous aggregation in solution (3). It is widely believed that the aggregation and accumulation of this peptide is involved in disease pathogenesis.

Aβ is produced primarily by neurons and secreted into the brain extracellular space where it is normally found in a soluble state (4). A variety of physiological processes, including those associated with neuronal activity, are related to Aβ synthesis and release into the extracellular space (5–7). Under normal physiological conditions and in AD patients, the concentration of Aβ in brain extracellular fluid (interstitial fluid, ISF and cerebrospinal fluid, CSF) is low (10^{-10} M–10^{-9} M) (8–12). This is important because in vitro studies suggest that the critical concentration for spontaneous aggregation of Aβ is in the μM range (13, 14). Therefore, Aβ concentrations in vivo would have to increase by at least three to four orders of magnitude for spontaneous aggregation to be feasible in the extracellular space. To span this large concentration gap, several potential mechanisms have been proposed. Effective concentration could be increased through membrane association (15–17), macromolecular crowding (18), specific interactions with protein complexes or chaperones, or specific covalent modifications (19–23).

If preformed aggregates are introduced into the extracellular space, these species can act as seeds for amyloid formation, propagating amyloid growth at lower concentrations than that required for seed formation (24). In this study, we explored the possibility that low concentrations of soluble Aβ can be taken up by cells and concentrated into acidic vesicles. The combination of low pH and high effective concentration in acidic vesicles appear to yield favorable conditions for the spontaneous aggregation of Aβ.

Results

Uptake of Human Aβ into Late Endosomes/Lysosomes. Aβ_{1-42} (250 nM) labeled with fluorescein isothiocyanate (FITC-Aβ_{1-42}) was incubated with a variety of cell types for 24 h and then imaged using confocal microscopy. Uptake of FITC-Aβ_{1-42} was observed in vesicles of SHSY5Y neuroblastoma cells (Fig. 1*A*) and murine cortical neurons (Fig. 1*B*), but not in human embryonic kidney (HEK293) cells (Fig. 1*C*). These observations, consistent with previously published findings (25), suggest cellular specificity in the uptake of FITC-Aβ_{1-42}. Because of the ease of growth and manipulation (relative to primary neuronal cultures), SHSY5Y cells were used to perform further studies. SHSY5Y cells, incubated with 250 nM of FITC-Aβ_{1-40}, FITC-scrambled-Aβ_{1-42}, or FITC alone, demonstrated vesicular uptake with FITC-Aβ_{1-40} (Fig. 1*F*) but not FITC-scrambled-Aβ_{1-42} (Fig. 1*E*) or FITC alone (Fig. 1*D*), suggesting a sequence-specific uptake mechanism. Uptake of tetramethylrhodamine-Aβ_{1-42} (TMR-Aβ_{1-42}) was similar to that seen with FITC-Aβ_{1-42} (Fig. 2 *A* and *D*, and *G*), indicating that uptake was not fluorophore-dependent. To identify the vesicles into which Aβ accumulated, TMR-Aβ_{1-42}-loaded SHSY5Y cells were co-stained with LysoTracker, 30 min before imaging. All vesicles

Author contributions: X.H., S.L.C., G.B., C.F., R.V.P., and J.-M.L. designed research; X.H. and S.L.C. performed research; X.H., S.L.C., C.F., R.V.P., and J.-M.L. analyzed data; and X.H., S.L.C., G.B., C.F., R.V.P., and J.-M.L. wrote the paper.

The authors declare no conflict of interest.

[1]X.H. and S.L.C. contributed equally to this work.

[2]To whom correspondence may be addressed at: Department of Biochemistry and Biophysics, Washington University School of Medicine, 660 South Euclid Avenue, Box 8231, St. Louis, MO 63110. E-mail: frieden@biochem.wustl.edu.

[3]To whom correspondence may be addressed at: Department of Neurology, Washington University School of Medicine, 660 South Euclid Avenue, Box 8111, St. Louis, MO 63110. E-mail: leejm@neuro.wustl.edu.

This article contains supporting information online at www.pnas.org/cgi/content/full/0911281106/DCSupplemental.

www.pnas.org/cgi/doi/10.1073/pnas.0911281106

Downloaded at Palestinian Territory, occupied on December 16, 2021

www.manaraa.com

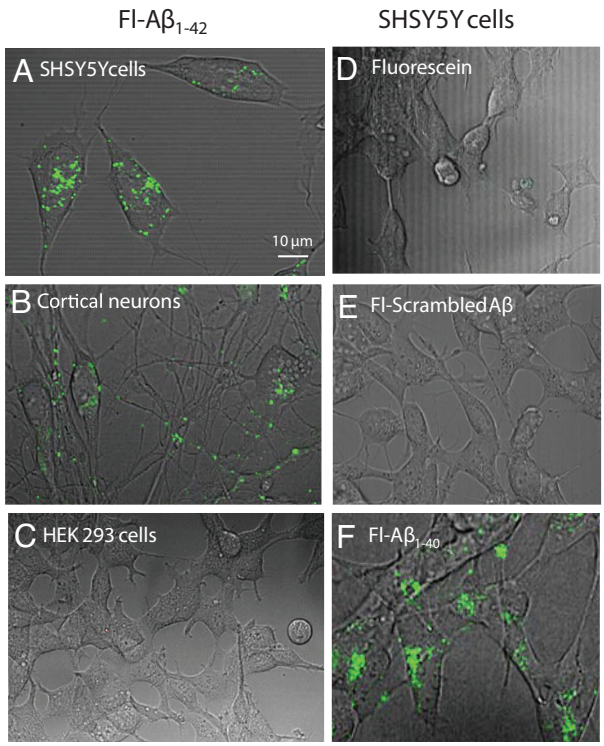

Fig. 1. Cell uptake of FITC-Aβ. (*A*) SHSY5Y cells, (*B*) primary murine cortical neurons, and (*C*) HEK293 cells were cultured in the presence of 250 nM human FITC-Aβ_{1-42} for 24 h, then imaged with confocal/phase-contrast microscopy. Vesicular uptake was observed only in the neurons and SHSY5Y cells. (*D*) SHSY5Y cells were incubated with 250 nM fluorescein alone, (*E*) FITC-scrambled Aβ_{1-42}, or (*F*) FITC-Aβ_{1-40} for 24 h. Vesicular uptake was observed with FITC-Aβ_{1-42} and Aβ_{1-40}, but not with FITC-scrambled-Aβ_{1-42} or fluorescein alone.

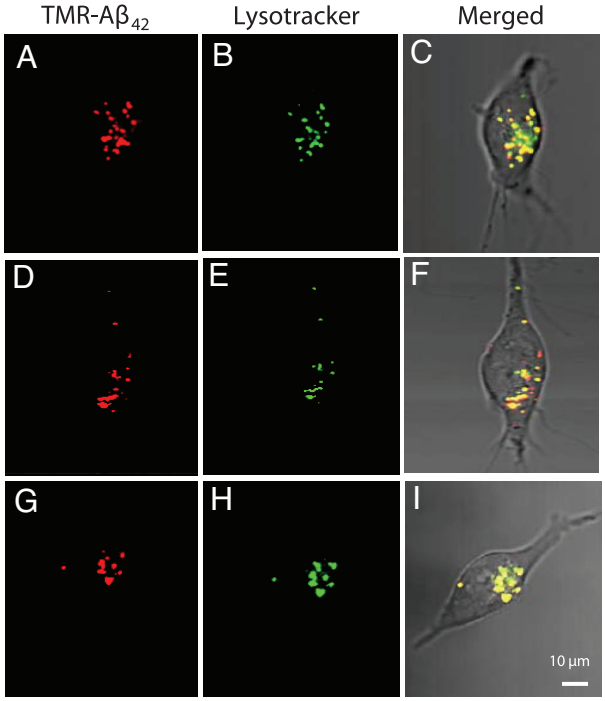

Fig. 2. Intracellular co-localization of Aβ_{1-42} with LysoTracker. SHSY5Y cells, grown in the presence of 250 nM TMR-Aβ_{1-42} for 24 h, were imaged 30 min after 50 nM LysoTracker was added to the culture medium. (*A, D,* and *G*) TMR-Aβ_{1-42} was detected in vesicles that co-stained with LysoTracker (*B, E,* and *H*); merged fluorescent images with phase contrast image (*C, F,* and *I*) demonstrate co-localization of Aβ and LysoTracker-stained vesicles.

with TMR-Aβ_{1-42} co-stained with LysoTracker and appeared to be a major subset of LysoTracker-positive vesicles (Fig. 2), suggesting that that Aβ is taken up and trafficked into late endosomes or lysosomally derived vesicles.

Because fluorescein fluorescence is altered at low pH, we chose to use TMR (which is relatively insensitive to pH changes) for more quantitative studies of Aβ_{1-42} uptake. TMR-Aβ_{1-42} uptake was both dose- (Fig. 3*A* and *B*) and time-dependent (Fig. 3*C* and Fig. S1*A*). Extracellular concentrations as low as 1 nM were sufficient to produce vesicular uptake within 24 h of incubation (Fig. 3*A*). Furthermore, fluorescent vesicles were first apparent within 2 h after the addition of 250 nM TMR-Aβ_{1-42} to cell cultures (Fig. 3*C* and Fig. S1*A*). Incubation with TMR alone did not result in cellular uptake throughout the concentration range examined (Fig. S1*B*). Furthermore, cell death was not detectable at all concentrations of TMR- Aβ_{1-42} examined (Fig. S2). To examine the fate of vesicular TMR-Aβ_{1-42}, after washout, SHSY5Y cells, loaded with TMR-Aβ for 24 h, were washed with medium free of TMR-Aβ. Within 24–48 h after wash-out, few fluorescent vesicles remained (Fig. 3*D* and Fig. S1*C*), suggesting rapid clearance/removal of TMR-Aβ after uptake and trafficking to late endosomes/lysosomes.

Concentration of Aβ_{1-42} in Vesicles. SHSY5Y cells, grown in the presence of 25 nM TMR-Aβ_{1-42} for 24 h, were imaged using confocal microscopy, and a pixel-by-pixel analysis of fluorescence intensity was performed to estimate the concentration of TMR-Aβ_{1-42} in vesicles. Fig. 4 shows fluorescence intensity on the *z* axis (in red) plotted above a high-power 2-D image of a group of SHSY5Y cells. To obtain a quantitative estimate of Aβ concentration inside the vesicles, pixel intensity was calibrated to known concentrations of free TMR (Fig. S3 *A* and *B*). Twenty-nine vesicles from five different images taken at random positions within the culture dish were analyzed. Vesicles, between 1–3 μm in diameter (consistent with late-endosomes/lysosomes), showed concentrations of TMR-Aβ_{1-42} between 1 and 2.5 μM. Two vesicles had concentrations well above 2.5 μM, although this is above the upper limit of detection with the instrumentation used. These data represent a concentration increase of approximately 100-fold from that originally added to the culture medium. As will be discussed, this is almost certainly an underestimate of the actual concentration inside the vesicles.

Vesicular Aβ_{1-42} Forms High Molecular Weight Aggregates. Given this approximately 100-fold difference in Aβ_{1-42} concentrations between the extracellular fluid and intracellular vesicles, SHSY5Y cells loaded with Aβ_{1-42} were examined for intracellular aggregates. SHSY5Y cells, grown in the presence of varying concentrations of unlabeled Aβ_{1-42} (0–1,000 nM) for 5 days or in the presence of 1 μM Aβ_{1-42} for varying periods of time (0–7 days), were washed, sonicated, and analyzed using agarose gel electrophoresis and immunoblotting with anti-Aβ antibodies (6E10 and 3D6, both N-terminal specific monoclonal antibodies). Tris-tricine gels showed high molecular weight (HMW) aggregates of Aβ (>200 kDa) in homogenates of cells grown in 1 μM Aβ_{1-42} for 5 days (Fig. 5*A*). Moreover, HMW aggregates (>800 kDa) were detected in cell homogenates in a concentration- (Fig. 5*B*) and time-dependent (Fig. 5*C*) manner, indicating that intracellular Aβ aggregation occurred only when cells were incubated with high extracellular concentrations of soluble Aβ. The HMW aggregates were recognized by two different anti-Aβ antibodies [6E10 (Fig. 5) and 3D6 (Fig. S4)]. Culture medium from these cells (containing 1 μM Aβ_{1-42}) did not show evidence

Downloaded at Palestinian Territory, occupied on December 16, 2021
www.manaraa.com

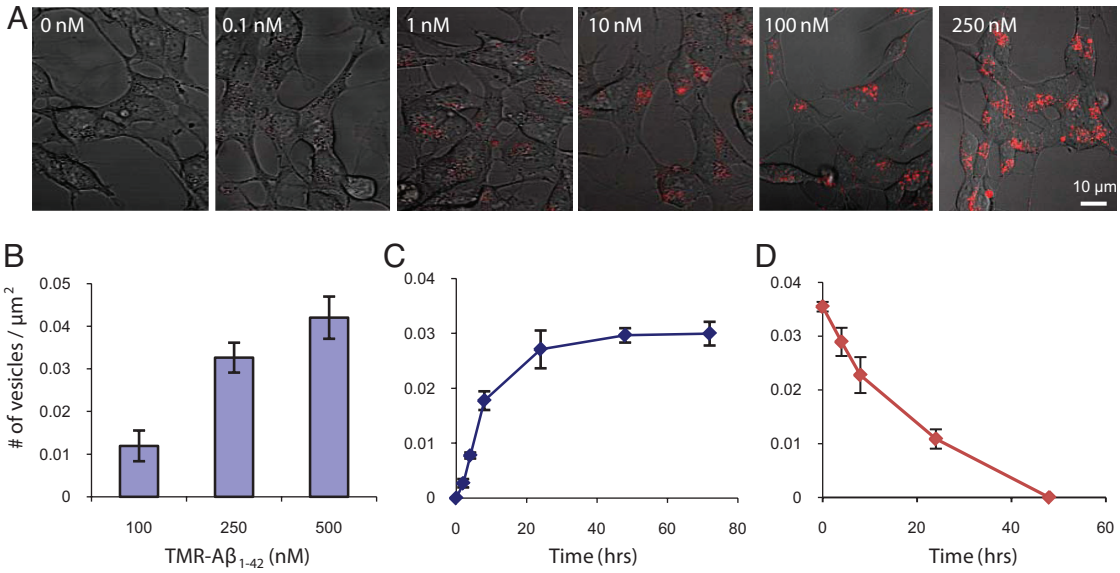

Fig. 3. Dose- and time-dependence of vesicular uptake of TMR-Aβ_{1-42}. SHSY5Y cells were grown in varying concentrations of TMR-labeled Aβ_{1-42} (1–250 nM as indicated (*A*), then imaged using confocal microscopy after 24 h. Fluorescent vesicles were quantified, and demonstrated dose-dependent uptake (*B*). SHSY5Y cells were grown in 250 nM TMR-Aβ_{1-42}, imaged at varying times (0–72 h) thereafter (Fig. S1 *A*), and fluorescent vesicles were quantified (*C*). SHSY5Y cells were grown in 250 nM TMR-Aβ_{1-42} for 24 h, TMR-Aβ_{1-42} was washed out of the medium, imaged a various times thereafter (Fig. S1C), and fluorescent vesicles were quantified (*D*). After washout, the number of fluorescent vesicles decreased with time, disappearing by 48 h. Error bars, s.e.m. from three independent experiments.

of aggregation in Tris-tricine (Fig. 5*A*, far left lane) or agarose gels (Fig. 5*D*, far right lane), consistent with previous reports that Aβ is less prone to aggregation in serum (26). Lower concentrations of extracellular Aβ_{1-42} (0–500 nM) did not result in intracellular aggregation during the 5-day incubation period (Fig. 5*B*). Intracellular aggregation appeared to increase with increasing incubation times appearing as early as 2 days (Fig. 5*C*). Interestingly, equivalent concentrations of extracellular human Aβ_{1-40} or rat Aβ_{1-42} did not elicit intracellular aggregation (Fig. 5*D*).

Intracellular Aβ_{1-42} Aggregates Can Seed Amyloid Fibril Formation. To determine whether HMW aggregates of Aβ that formed in intracellular vesicles can seed the formation of amyloid fibrils, control cells, cells loaded with unlabeled Aβ_{1-42}, and cells incubated with scrambled Aβ_{1-42} were sonicated with SDS, and homogenates were incubated with 100 nM TMR-Aβ_{1-42} at 37 °C for 48 h. This concentration of Aβ is too low for spontaneous formation of fibrils within this time frame. Aβ-loaded cell extracts induced the appearance of fluorescent precipitates, visible by microscopy (Fig. 6*E*), while extracts from cells grown in the absence of Aβ (Fig. 6*D*) or in the presence of scrambled-Aβ (Fig. 6*F*) did not. Moreover, these same precipitates stained with Thioflavin-S, suggesting the formation of fibrils (Fig. 6*H*). Again, extracts from cells grown in the absence of Aβ (Fig. 6*G*) or in the presence of scrambled-Aβ (Fig. 6*I*) failed to develop Thioflavin-S staining. Moreover, fresh Aβ-loaded cell extract (before incubation with free Aβ) did not show Thioflavin-S staining.

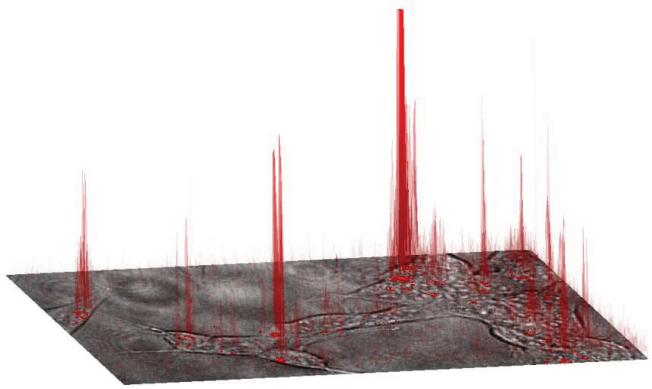

Fig. 4. SHSY5Y cells, grown in the presence of 25 nM TMR-Aβ_{1-42} for 24 h, were imaged using confocal microscopy. The phase image of a group of cells is shown in the x-y plane with the fluorescence intensity plotted on the *z* axis and projected onto the image. The fluorescence originating from intracellular vesicles is up to two orders of magnitude greater than fluorescence in the extracellular medium (see Fig. S3 *A* and *B*), suggesting high effective concentrations of Aβ in the vesicles.

Discussion

A major conundrum in understanding spontaneous appearance of plaques in the AD brain is the gap between known extracellular Aβ concentrations in vivo (in the low nM range) and the concentration required for spontaneous aggregation in vitro (which is in the μM range). This concentration gap spans three to four orders of magnitude. In this study, we find that SHSY5Y neuroblastoma cells and cortical neurons are capable of taking up and concentrating extracellular Aβ even at low, physiologically relevant concentrations. Starting with an extracellular concentration of 25 nM, we estimated the concentrations inside some intracellular vesicles to be at least 2.5 μM. However, this is a likely a conservative estimate for several reasons. First, it is likely that the high concentrations within vesicles result in quenching of TMR fluorescence. Second, because fluorescent intensities were quantified in a single 2-D plane, it is unlikely that vesicles were entirely contained within the confocal beam volume. Off-target vesicles will result in concentration underestimations because fluorescence intensity decays as e^{-r^2} where r is the radial distance from the point of maximal intensity. Third, our concentration calibration was performed on a homogeneous solution of fluorophores, under the assumption of uniform filling of the beam volume. Under experimental conditions, it is likely that

Downloaded at Palestinian Territory, occupied on December 16, 2021
www.manaraa.com

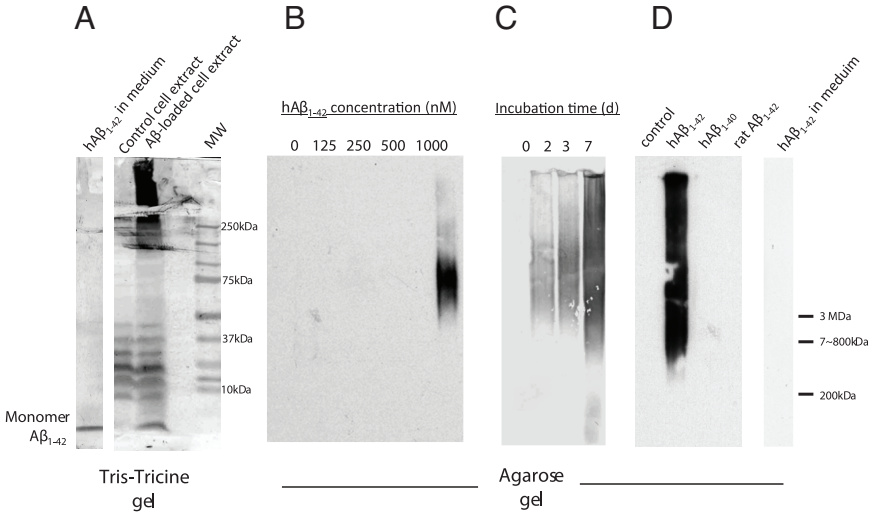

Fig. 5. Aggregation of intracellular Aβ_{1-42} into HMW forms. (*A*) SHSY5Y cells, grown in the presence or absence of Aβ_{1-42} (1 μM) for 5 days, were homogenized and run on a Tris-Tricine gel and blotted with an anti-Aβ antibody (6E10). Culture medium incubated with Aβ_{1-42} (1 μM) for 5 days show the presence of only monomers. Extracts from cells grown in Aβ_{1-42} show HMW aggregates, while cell grown without Aβ do not (note the non-specific bands in the 10–40 kDa range from the cell extracts). (*B–D*) SHSY5Y cells were grown in the presence of Aβ_{1-42} (0–1,000 nM as indicated) for 5 days (*B*), for varying times (0–7 days, 1 μM Aβ) (*C*), or in the presence of human Aβ_{1-42}, Aβ_{1-40}, or rat Aβ_{1-42} for 5 days (as indicated in *D*). Cell homogenates were then run on an agarose gel and blotted with an anti-Aβ antibody (6E10). Intracellular Aβ was found to aggregate in a concentration- and time-dependent manner. Human Aβ_{1-42} forms HMW intracellular aggregates, but human Aβ_{1-40} and rat Aβ_{1-42} do not. Human Aβ_{1-42} incubated in culture medium alone for 5 days did not form HMW aggregates (*D*, right lane).

a large number of fluorophores are contained within a volume smaller than that defined by a single pixel; this may be especially pronounced in an aggregate. Therefore, assuming the fluorophores are uniformly filling the beam volume can only lead to an underestimation. Finally, it is likely that the final concentration of Aβ added to the culture medium decreases with time due to the release of Aβ-degrading proteases into the culture medium by neural cells (27). Therefore, it is likely that the concentrations of Aβ in the intracellular vesicles may, in fact, be an order of magnitude higher than what we have estimated. This is in line with estimates of the critical concentration that support spontaneous aggregation of Aβ (28). Therefore, we propose that certain cells may be capable of taking up Aβ and increasing its effective concentration by several orders of magnitude.

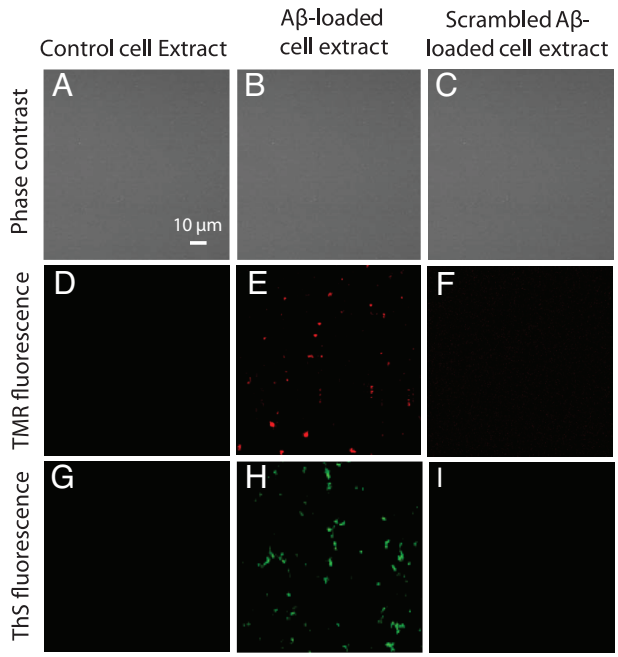

Fig. 6. Cell extracts from Aβ_{1-42}-loaded cells seed the formation of amyloid fibrils. SHSY5Y cells incubated with or without 1 μM unlabeled Aβ_{1-42} or scrambled Aβ_{1-42} for 5 days were homogenized and then incubated with 100 nM TMR-Aβ_{1-42} for 48 h. Phase contrast images of the cell extracts show the absence of cells (*A–C*). Extracts from control cells (grown in the absence of Aβ) did not show TMR fluorescence (*D*) or Thioflavin-S staining (*G*); Aβ-loaded cell extracts developed TMR precipitates (*E*) which stained for Thioflavin-S (*H*); while scrambled-Aβ-loaded cell extracts showed neither (*F* and *I*). These results suggest that intracellular Aβ aggregates can seed the formation of Thioflavin-positive aggregates.

Most estimates for the concentration of Aβ in human cerebrospinal fluid (CSF) have been in the low nM range (0.1–1 nM) (8–12). Although CSF concentrations of proteins do not necessarily reflect interstitial fluid (ISF) concentrations (the more relevant quantity), a recent study examining Aβ levels in human head trauma patients using microdialysis suggested that the concentration of Aβ is similar in the two pools (29). At nM concentrations, it is believed that Aβ exists in soluble form, either as a monomer or low molecular weight oligomer (30). Although intracellular aggregation was not detected when cells were incubated with extracellular Aβ at concentrations below 1 μM, it must be noted that the time-line for the experiments was 5 days. It is likely that in vivo (during human disease pathogenesis) the time frame for accumulation of intracellular Aβ could be on the order of years to decades. Thus, a small imbalance in vesicular accumulation/degradation could lead to large increases in effective concentrations over the span of years and decades. Our in vitro experiments were designed to accelerate this process using higher concentrations of extracellular Aβ (1 μM). Furthermore, this concentration differential between uptake and that required for aggregation underscores one of the major implications of this study: that uptake of Aβ occurs at physiologically relevant extracellular concentrations (1–10 nM), while intravesicular Aβ aggregation requires higher concentrations (1 μM, extracellular). We demonstrate that this concentration differential can be achieved via a vesicular concentrating step involving a two to three order of magnitude increase in Aβ concentration. Previous studies have shown that high concen-

Downloaded at Palestinian Territory, occupied on December 16, 2021
www.manaraa.com

trations of Aβ under acidic conditions (including those found in endosomal compartments) favor rapid aggregation (31, 32).

There is growing evidence that Aβ accumulates in vesicles in neurons before the development of amyloid plaques. In a variety of AD mouse models, vesicular Aβ immunostaining has been observed in cortical and hippocampal neurons before the deposition of amyloid plaques (33, 34). Such vesicular Aβ immunostaining is absent in wildtype controls. Similar vesicular Aβ immunostaining has been reported in human AD brains (35, 36), in AD-vulnerable brain regions from non-demented individuals, and in brains of young Down's Syndrome cases before the deposition of plaques (35, 37). Although it has been speculated that this vesicular Aβ represents new Aβ synthesis from APP processing, an equally likely possibility is that this pool represents extracellular Aβ taken up by cells. Our studies focus on cellular uptake of Aβ and do not address cell-autonomous APP processing and Aβ synthesis.

The specific uptake of $A\beta_{1-40}$ and $A\beta_{1-42}$, but not scrambled-Aβ, suggests that the uptake mechanism in SHSY5Y cells is receptor-mediated rather than via a non-specific mechanism like bulk uptake (TMR uptake was not observed). Although several Aβ-binding receptors have been reported, the low density lipoprotein receptor-like protein-1 (LRP1) is likely a major neuronal Aβ receptor (38). LRP1 can bind Aβ either directly (39) or via Aβ chaperones such as apoE (40). A role for LRP1 in neuronal Aβ uptake is supported by a study demonstrating that TGFβ2-mediated intraneuronal accumulation of brain injected Aβ is markedly inhibited by LRP1 antagonist RAP (41). Interestingly, HEK293 cells, which poorly internalized Aβ in this study, express very low levels of LRP1. The cellular uptake mechanisms that lead to intraneuronal Aβ accumulation require further investigation.

Why would Aβ be taken up and trafficked to endosomes/lysosomes? The wash-out studies demonstrate that vesicular Aβ rapidly disappears after Aβ is washed out of the culture medium, suggesting an efficient clearance mechanism. However, when continuously exposed to extracellular Aβ, vesicular Aβ accumulates. As vesicular Aβ concentrations increase, it is possible that the degradative capacity of the endosomal/lysosomal pathway may be overwhelmed, leading to the accumulation of Aβ. Such accumulation may result in aggregation, with Aβ aggregates being degraded less efficiently than monomer or small oligomers (42). Thus, one might speculate that disruption of this intracellular degradative pathway might lead to enhanced seed formation, and therefore more plaque deposition. In fact, gene deletion of a major lysosomal protease known to degrade Aβ, cathepsin B, resulted in a dramatic increase in plaque pathogenesis (43). Conversely, gene deletion of an endogenous inhibitor of cathepsin, cystatin C, reduced amyloid plaque load (44), and this effect was eliminated in cathepsin B-knockout mice (43). These studies add support to the idea that lysosomal proteolytic activity influences amyloid plaque pathogenesis.

Our data suggest that there is a difference between the aggregating behavior of $A\beta_{1-40}$ and $A\beta_{1-42}$ even though both molecules are trafficked into the endosomes/lysosomes. In vitro experiments indicate that the critical concentration for $A\beta_{1-40}$ aggregation is higher than that of $A\beta_{1-42}$ (3). This leads to the interesting possibility that aggregation protects $A\beta_{1-42}$ molecules from degradation in endosomes/lysosomes cleavage, whereas the competition between aggregation and degradation favors the latter for $A\beta_{1-40}$. If $A\beta_{1-42}$ molecules form aggregates that are less efficiently degraded in lysosomally-derived vesicles, then these aggregates could accumulate within cells. It is conceivable that these aggregates could then be released into the extracellular space either through, active exocytotic mechanisms, or through stress-induced cell death. Future studies will focus on in-vesicle aggregation and the fate of these aggregates so we may assess their role in aggregation-mediated pathogenesis in AD.

Materials and Methods

Reagents. $A\beta_{1-42}$ and $A\beta_{1-40}$ (American Peptide); FITC-$A\beta_{1-42}$ and FITC-scrambled-$A\beta_{1-42}$ (rpeptide); TMR, TMR-scrambled-Aβ, and TMR-$A\beta_{1-42}$ (Anaspec);. fluorescein, trifluoroacetic acid, and 1,1,1,3,3,3-hexafluoro-2-propanol (Sigma); LysoTracker Green DND-26 (Molecular Probes); 6E10 antibody (Sigma); and 3D6 antibody (generous gift from Eli Lilly to G.B.).

Aβ Preparation: $A\beta_{1-42}$ and $A\beta_{1-40}$. Dry peptide (1 mg) was pretreated with neat trifluoroacetic acid (1 mL), distilled under nitrogen, washed with 1,1,1,3,3,3-hexafluoro-2-propanol (1 mL), distilled under nitrogen, then dissolved in DMSO to 200 μM, and stored at -20 °C.

Cell Culture and Cellular Uptake. All cells were grown in Dulbeco's modified eagle medium (DMEM) supplemented with 10% (vol/vol) FBS. Murine cortical neurons derived from embryonic day 15.5 mice were grown in BME medium (with 5% horse serum and 5% FBS) and treated with cytosine β-D-arabinofuranoside hydrochloride (4 μg/mL) at 1 day. In neurons, 250 nM FITC-$A\beta_{1-42}$ was added after 7 days in vitro and incubated for 24 h. FITC-$A\beta_{1-42}$, FITC- $A\beta_{1-40}$, FITC-scrambled-$A\beta_{1-42}$, and free fluorescein, were added to SHSY5Y cultures for 24 h. For time-dependence experiments, 250 nM TMR-$A\beta_{1-42}$ was added to SHSY5Y cells, plated in 8-well Lab-Tek chamber slides (Nunc) and images (Zeiss) were acquired at varying times (0–72 h) after addition of the labeled-$A\beta_{1-42}$. For dose-dependence experiments, TMR-$A\beta_{1-42}$ was added at varying concentrations (0–250 nM) and imaged 24 h thereafter. SHSY5Y cells grown in 250 nM TMR-$A\beta_{1-42}$ for 24 h were stained with LysoTracker Green (50 nM) for 30 min before confocal imaging.

Fluorescence Intensity Quantification. SHSY5Y cells incubated with 25 nM TMR-$A\beta_{1-42}$ for 24 h were imaged using the confocal microscope (at 543 nm excitation, 560–615 nm bandpass emissions; 40× water immersion objective). Pixel intensity at different laser powers was calibrated using known concentrations of free TMR (Fig. S3 *A* and *B*). Six images from random regions of the culture dish were analyzed at five different excitation laser powers. In each image, four to five fluorescent vesicles, of size consistent with lysosomes (1–3 μm in diameter), were selected inside different cells. For each point, four adjacent pixels centered about the most intense region of the vesicle were analyzed. The mean brightness was calculated and compared to the calibration curves to determine the concentration (Fig. S3 *A* and *B*).

Cell Death Assay. Lactate Dehydrogenase (LDH) activity released into culture media by dying cells was assessed as an index of cell death, as previously described (45).

Immunoblot. SHSY5Y cells were washed twice with cold PBS and detached with 0.05% trypsin/0.02%. The cell pellet was resuspended in cold Hanks' balanced salt solution (HBSS buffer), sonicated (Fisher Scientific) at level 3 using 1-s pulses × 10, and centrifuged at 3,000 × *g* for 5 min. The supernatant was loaded onto a 16.5% Tris-Tricine gel, transferred to a polyvinylidene difluoride (PVDF) membrane and probed with monoclonal antibody 6E10.

Agarose Gel Electrophoresis. Agarose (1.5% wt/vol) was melted in running buffer (20 mM Tris and 200 mM glycine) without SDS. While stirring the melted agarose, 10% (wt/vol) SDS solution was added (drop by drop to avoid local solidification of the agarose) to a 0.1% final SDS concentration. Cell extract was incubated for 7 min in sample buffer [60 mM Tris-HCl (pH 6.8), 5% glycerol, 2% SDS, and 0.05% bromophenol blue] at room temperature, resolved in a horizontal 1.5% agarose gel in a standard Tris/glycine/SDS buffer, transferred electrophoretically to a PVDF membrane, and probed with 6E10 or 3D6.

In Vitro Seeding. SHSY5Y cell pellets were resuspended in 2% SDS in PBS, sonicated (as above), and diluted 1:40 in PBS with 0.02% sodium azide and loaded into Labtek 8-well chambers to a final SDS concentration of 0.05%. 100 nM TMR-$A\beta_{1-42}$ was then added, and after incubation at 37 °C for 48 h, images were acquired by fluorescence microscopy.

Thioflavin-S Staining. Culture wells were washed and incubated with 0.025% Thioflavin-S solution (in 50% ethanol) for 5 min, rinsed with 50% ethanol and water, and cover slipped for imaging.

ACKNOWLEDGMENTS. Support was provided by the National Institutes of Health grants R01 NS48283, R01 NS67905, and P01 NS32636 (to J.-M.L.); R01 AG027924 (to G.B.); R01 DK13332 (to C.F.); and R01 NS056114 (to R.V.P.); and Washington University's Hope Center for Neurological Disorders (to J.-M.L.).

Downloaded at Palestinian Territory, occupied on December 16, 2021

www.manaraa.com

1. Glenner GG, Wong CW (1984) Alzheimer's disease: Initial report of the purification and characterization of a novel cerebrovascular amyloid protein. *Biochem Biophys Res Commun* 120:885–890.
2. Halverson K, Fraser PE, Kirschner DA, Lansbury PT, Jr (1990) Molecular determinants of amyloid deposition in Alzheimer's disease: Conformational studies of synthetic beta-protein fragments. *Biochemistry* 29:2639–2644.
3. Snyder SW, et al. (1994) Amyloid-beta aggregation: Selective inhibition of aggregation in mixtures of amyloid with different chain lengths. *Biophys J* 67:1216–1228.
4. Sisodia SS (1992) Secretion of the beta-amyloid precursor protein. *Ann N Y Acad Sci* 674:53–57.
5. Walsh DM, et al. (2002) Naturally secreted oligomers of amyloid beta protein potently inhibit hippocampal long-term potentiation in vivo. *Nature* 416:535–539.
6. Cirrito JR, et al. (2003) In vivo assessment of brain interstitial fluid with microdialysis reveals plaque-associated changes in amyloid-beta metabolism and half-life. *J Neurosci* 23:8844–8853.
7. Cirrito JR, et al. (2005) Synaptic activity regulates interstitial fluid amyloid-beta levels in vivo. *Neuron* 48:913–922.
8. Seubert P, et al. (1992) Isolation and quantification of soluble Alzheimer's beta-peptide from biological fluids. *Nature* 359:325–327.
9. Galasko D, et al. (1998) High cerebrospinal fluid tau and low amyloid beta42 levels in the clinical diagnosis of Alzheimer disease and relation to apolipoprotein E genotype. *Arch Neurol* 55:937–945.
10. Andreasen N, et al. (1999) Cerebrospinal fluid beta-amyloid(1–42) in Alzheimer disease: Differences between early- and late-onset Alzheimer disease and stability during the course of disease. *Arch Neurol* 56:673–680.
11. Strozyk D, Blennow K, White LR, Launer LJ (2003) CSF Abeta 42 levels correlate with amyloid-neuropathology in a population-based autopsy study. *Neurology* 60:652–656.
12. Gustafson DR, Skoog I, Rosengren L, Zetterberg H, Blennow K (2007) Cerebrospinal fluid beta-amyloid 1–42 concentration may predict cognitive decline in older women. *J Neurol Neurosurg Psychiatry* 78:461–464.
13. Lomakin A, Teplow DB, Kirschner DA, Benedek GB (1997) Kinetic theory of fibrillogenesis of amyloid beta-protein. *Proc Natl Acad Sci USA* 94:7942–7947.
14. Harper JD, Wong SS, Lieber CM, Lansbury PT, Jr (1999) Assembly of A beta amyloid protofibrils: An in vitro model for a possible early event in Alzheimer's disease. *Biochemistry* 38:8972–8980.
15. Gorbenko GP, Kinnunen PK (2006) The role of lipid-protein interactions in amyloid-type protein fibril formation. *Chem Phys Lipids* 141:72–82.
16. Matsuzaki K (2007) Physicochemical interactions of amyloid beta-peptide with lipid bilayers. *Biochim Biophys Acta* 1768:1935–1942.
17. Aisenbrey C, et al. (2008) How is protein aggregation in amyloidogenic diseases modulated by biological membranes? *Eur Biophys J* 37:247–255.
18. Munishkina LA, Cooper EM, Uversky VN, Fink AL (2004) The effect of macromolecular crowding on protein aggregation and amyloid fibril formation. *J Mol Recognit* 17:456–464.
19. Eriksson S, Janciauskiene S, Lannfelt L (1995) Alpha 1-antichymotrypsin regulates Alzheimer beta-amyloid peptide fibril formation. *Proc Natl Acad Sci USA* 92:2313–2317.
20. Cotman SL, Halfter W, Cole GJ (2000) Agrin binds to beta-amyloid (Abeta), accelerates abeta fibril formation, and is localized to Abeta deposits in Alzheimer's disease brain. *Mol Cell Neurosci* 15:183–198.
21. Castillo GM, Ngo C, Cummings J, Wight TN, Snow AD (1997) Perlecan binds to the beta-amyloid proteins (A beta) of Alzheimer's disease, accelerates A beta fibril formation, and maintains A beta fibril stability. *J Neurochem* 69:2452–2465.
22. Snow AD, et al. (1994) An important role of heparan sulfate proteoglycan (Perlecan) in a model system for the deposition and persistence of fibrillar A beta-amyloid in rat brain. *Neuron* 12:219–234.
23. Smith DG, Cappai R, Barnham KJ (2007) The redox chemistry of the Alzheimer's disease amyloid beta peptide. *Biochim Biophys Acta* 1768:1976–1990.
24. Harper JD, Lansbury PT, Jr (1997) Models of amyloid seeding in Alzheimer's disease and scrapie: Mechanistic truths and physiological consequences of the time-dependent solubility of amyloid proteins. *Ann Rev Biochem* 66:385–407.
25. Knauer MF, Soreghan B, Burdick D, Kosmoski J, Glabe CG (1992) Intracellular accumulation and resistance to degradation of the Alzheimer amyloid A4/beta protein. *Proc Natl Acad Sci USA* 89:7437–7441.
26. Biere AL, et al. (1996) Amyloid beta-peptide is transported on lipoproteins and albumin in human plasma. *J Biol Chem* 271:32916–32922.
27. Yin KJ, et al. (2006) Matrix metalloproteinases expressed by astrocytes mediate extracellular amyloid-beta peptide catabolism. *J Neurosci* 26(43):10939–10948.
28. Huang TH, Yang DS, Fraser PE, Chakrabartty A (2000) Alternate aggregation pathways of the Alzheimer beta-amyloid peptide. An in vitro model of preamyloid. *J Biol Chem* 275:36436–36440.
29. Brody DL, et al. (2008) Amyloid-beta dynamics correlate with neurological status in the injured human brain. *Science* 321:1221–1224.
30. Sengupta P, et al. (2003) The amyloid beta peptide (Abeta(1–40)) is thermodynamically soluble at physiological concentrations. *Biochemistry* 42:10506–10513.
31. Burdick D, et al. (1992) Assembly and aggregation properties of synthetic Alzheimer's A4/beta amyloid peptide analogs. *J Biol Chem* 267:546–554.
32. Gorman PM, Yip CM, Fraser PE, Chakrabartty A (2003) Alternate aggregation pathways of the Alzheimer beta-amyloid peptide: Abeta association kinetics at endosomal pH. *J Mol Biol* 325:743–757.
33. Wirths O, et al. (2001) Intraneuronal Abeta accumulation precedes plaque formation in beta-amyloid precursor protein and presenilin-1 double-transgenic mice. *Neurosci Lett* 306:116–120.
34. Oddo S, et al. (2003) Triple-transgenic model of Alzheimer's disease with plaques and tangles: Intracellular Abeta and synaptic dysfunction. *Neuron* 39:409–421.
35. Gouras GK, et al. (2000) Intraneuronal Abeta42 accumulation in human brain. *Am J Pathol* 156:15–20.
36. LaFerla FM, Green KN, Oddo S (2007) Intracellular amyloid-beta in Alzheimer's disease. *Nat Rev* 8:499–509.
37. Gyure KA, Durham R, Stewart WF, Smialek JE, Troncoso JC (2001) Intraneuronal abeta-amyloid precedes development of amyloid plaques in Down syndrome. *Arch Pathol Lab Med* 125:489–492.
38. Zerbinatti CV, Bu G (2005) LRP and Alzheimer's disease. *Rev Neurosci* 16:123–135.
39. Deane R, et al. (2004) LRP/amyloid beta-peptide interaction mediates differential brain efflux of Abeta isoforms. *Neuron* 43:333–344.
40. Zerbinatti CV, et al. (2006) Apolipoprotein E and low density lipoprotein receptor-related protein facilitate intraneuronal Abeta42 accumulation in amyloid model mice. *J Biol Chem* 281:36180–36186.
41. Harris-White ME, et al. (2004) Role of LRP in TGFbeta2-mediated neuronal uptake of Abeta and effects on memory. *J Neurosci Res* 77(2):217–228.
42. Soto C, Castano EM (1996) The conformation of Alzheimer's beta peptide determines the rate of amyloid formation and its resistance to proteolysis. *Biochem J* 314:701–707.
43. Mueller-Steiner S, et al. (2006) Antiamyloidogenic and neuroprotective functions of cathepsin B: Implications for Alzheimer's disease. *Neuron* 51:703–714.
44. Mi W, et al. (2007) Cystatin C inhibits amyloid-beta deposition in Alzheimer's disease mouse models. *Nat Genet* 39:1440–1442.
45. Xu J, et al. (2000) Oxygen-Glucose Deprivation Induces Inducible Nitric Oxide Synthase and Nitrotyrosine Expression in Cerebral Endothelial Cells. *Stroke* 31:1744–1751.

Downloaded at Palestinian Territory, occupied on December 16, 2021

www.manaraa.com